Magnon Landau Levels and Emergent Supersymmetry in Strained Antiferromagnets

Mary Madelynn Nayga,[1,2] Stephan Rachel,[3] and Matthias Vojta[1]
[1]Institut für Theoretische Physik and Würzburg-Dresden Cluster of Excellence ct.qmat, Technische Universität Dresden, 01062 Dresden, Germany
[2]Max-Planck-Institut für Chemische Physik fester Stoffe, Nöthnitzer Straße 40, 01187 Dresden, Germany
[3]School of Physics, University of Melbourne, Parkville, VIC 3010, Australia

(Received 19 March 2019; published 15 November 2019)

Inhomogeneous strain applied to lattice systems can induce artificial gauge fields for particles moving on this lattice. Here we demonstrate how to engineer a novel state of matter, namely an antiferromagnet with a Landau-level excitation spectrum of magnons. We consider a honeycomb-lattice Heisenberg model and show that triaxial strain leads to equally spaced pseudo-Landau levels at the upper end of the magnon spectrum, with degeneracies characteristic of emergent supersymmetry. We also present a particular strain protocol which induces perfectly quantized magnon Landau levels over the whole bandwidth. We discuss experimental realizations and generalizations.

DOI: 10.1103/PhysRevLett.123.207204

Introduction.—Artificial gauge fields have become a powerful tool for engineering states of matter. Originally discussed in the context of strain applied to carbon nanotubes [1], they later were utilized to induce Landau levels in strained graphene [2–5], with a spacing corresponding to a magnetic field exceeding 300 T, far beyond what is reachable with laboratory magnetic fields. More fundamentally, artificial gauge fields can be used to induce effects akin to that of orbital magnetic fields for *charge-neutral* particles, resulting in novel states which cannot be generated otherwise. This has been proposed for ultracold gases as well as solids [6,7], with strain-induced Landau levels for Bogoliubov quasiparticles of nodal superconductors [8,9] and for Majorana excitations of a Kitaev spin liquid [10] being two prominent examples.

In this Letter, we propose a novel setting for strain engineering, namely ordered quantum antiferromagnets. We show that inhomogeneous exchange couplings in simple Néel antiferromagnets, generated by applying a suitable strain pattern, transform the conventional magnon spectrum into a sequence of magnonic pseudo-Landau levels. There are three key differences to previous condensed-matter realizations of pseudo-Landau levels: (i) The magnon Landau levels emerge in the high-energy part of the spectrum, i.e., starting from the upper band edge, not at low energies as in the graphene case. (ii) The magnon Landau levels derive from a mode which disperses quadratically in the absence of strain, not from a linear Dirac-like dispersion. As a result, the magnon Landau levels are equally spaced, with a spacing scaling linearly with the pseudomagnetic field, as opposed to the square-root dependence of Dirac Landau levels. (iii) Perhaps most remarkably, the Landau-level spectrum displays emergent supersymmetry: Its degeneracies are equivalent to that of a system with a boson and a fermion of equal energy, thus forming one of the rare condensed-matter realizations of supersymmetry [11–13], which in general refers to systems where each boson has a fermionic superpartner and vice versa.

We present numerical spin-wave results for the Heisenberg antiferromagnet on finite honeycomb lattices subject to triaxial strain, Fig. 1(a), and we derive the corresponding continuum field theory which is based on an expansion about the *maximum* of the magnon dispersion. Following earlier work [14], we also show that the combined limit of strong magnetoelastic coupling and weak lattice deformations leads to perfectly quantized magnon Landau levels over the entire range of magnon energies. We argue that magnon Landau levels can be detected in high-resolution spectroscopic experiments on strained honeycomb antiferromagnets, and we discuss generalizations to other lattices.

We note that very different types of magnon Landau levels have appeared in earlier work. Reference [15] considered gapped antiferromagnets subject to electric field gradients, and Ref. [16] studied Dirac magnons in ferromagnets under strain.

Model and spin-wave theory.—We consider a standard nearest-neighbor antiferromagnetic Heisenberg model of spins S placed on the sites of a honeycomb lattice. The Hamiltonian with spatially varying couplings reads

$$\mathcal{H} = \sum_{\langle ij \rangle} J_{ij} \vec{S}_i \cdot \vec{S}_j. \tag{1}$$

On this bipartite lattice, the antiferromagnetic couplings are unfrustrated, such that the ground state of the homogeneous system, $J_{ij} \equiv J$, is a simple Néel antiferromagnet for any S. In the following we will assume that a Néel state is

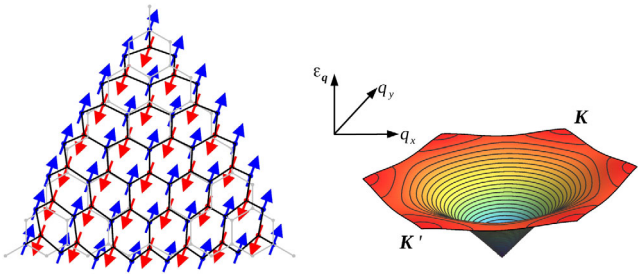

FIG. 1. Left: distorted honeycomb-lattice antiferromagnet, with displacements from triaxial strain, Eq. (4); the undistorted lattice is shown in light gray. Longer (shorter) bonds correspond to weaker (stronger) exchange couplings J_{ij}. The system size is $N = 8$. Right: magnon spectrum of the unstrained honeycomb Heisenberg antiferromagnet, showing a quadratic maximum at momenta $\vec{K}$ and $\vec{K}'$.

also realized in the strained system; this applies in the semiclassical ($S \to \infty$) limit [17] as well as, by continuity, for weak strain and any S.

The excitation spectrum can be obtained using spin-wave (SW) theory. Using Holstein-Primakoff bosons a and b on sublattices A and B, respectively, which describe fluctuations above the collinear Néel state, the bilinear piece of the Hamiltonian reads

$$\mathcal{H}_{\mathrm{SW}} = S\sum_{\langle ij\rangle} J_{ij}(a_i^\dagger a_i + b_j^\dagger b_j + a_i b_j + a_i^\dagger b_j^\dagger). \quad (2)$$

In the homogeneous (i.e., unstrained) case, the Hamiltonian can be transformed by subsequent Fourier and Bogoliubov transformations into a system of noninteracting bosons with energies

$$\omega_{\vec{q}} = 3JS\sqrt{1 - |\gamma_{\vec{q}}|^2} \quad (3)$$

where $\gamma_{\vec{q}} = (1/3)\sum_j e^{i\vec{q}\cdot\vec{\delta}_j}$ with $\vec{\delta}_j$ being the three nearest-neighbor vectors on the honeycomb lattice. This spectrum displays gapless (Goldstone) modes at $\vec{q} = 0$ and is maximum at the momenta $\vec{q} = \vec{K} = 2\pi/(3a_0)(1/\sqrt{3}, 1)$ and $\vec{K}' = -2\pi/(3a_0)(1/\sqrt{3}, 1)$, with a_0 the lattice constant, Fig. 1(b).

Strain-induced Landau levels.—In the context of graphene, it has been theoretically shown [2,5] that a spatial modulation of hopping energies mimics the effect of a vector potential. Near the Dirac energy, this emergent vector potential can be expressed through the strain tensor u_{ij} as $\vec{A} \propto \pm(u_{xx} - u_{yy}, -2u_{xy})^T$. If the resulting pseudomagnetic field, $\vec{B} = \mathrm{rot}\vec{A}$, is sufficiently homogeneous—this applies, e.g., to triaxial strain with the displacement vector given by [2,18]

$$\vec{U}(x, y) = \bar{C}(2xy, x^2 - y^2)^T; \quad (4)$$

it can induce single-particle pseudo-Landau levels very similar to Landau levels in a physical magnetic field. In Eq. (4) $\bar{C}$ (measured in units of $1/a_0$) parametrizes the distortion, and $u_{ij} = (\partial_i U_j + \partial_j U_i)/2$.

Adapting the idea of strain-induced artificial gauge fields to antiferromagnets, we shall study the Heisenberg model (1) with spatially modulated exchange couplings. We choose

$$J_{ij} = J[1 - \beta(|\vec{\delta}_{ij}|/a_0 - 1)] \quad (5)$$

where we calculate the distance $\vec{\delta}_{ij} = \vec{R}_i + \vec{U}_i - \vec{R}_j - \vec{U}_j$ using the displacement $\vec{U}(x, y)$ evaluated at the lattice positions $\vec{R}_i$ of the undistorted honeycomb lattice. The factor β encodes the strength of magnetoelastic coupling, and the dimensionless parameter (dubbed "strain" below) $C = \bar{C}\beta a_0$ will enter our simulations as a measure of the modulations of the J_{ij}. Note that Eq. (5) represents a linear approximation to the full dependence of the exchange constant on the bond length [18].

The inhomogeneous Heisenberg model (1) with couplings given by Eq. (5) is expected to display magnon excitations (on top of its collinear ground state) which are influenced by artificial gauge fields. As we demonstrate now, triaxial strain (4) will produce a homogeneous pseudomagnetic field for magnons with momenta near $\vec{K}$ and $\vec{K}'$ leading to equidistant pseudo-Landau levels.

Field theory for strained magnons.—We derive a continuum field theory which captures the effect of the strain-induced gauge field. To this end, we expand the magnon Hamiltonian near $\vec{K}$. We introduce the two-vector $\Psi(\vec{r}) = (\psi_a(\vec{r}), \psi_b^\dagger(\vec{r}))^T$, representing the real-space Fourier transform of $(a_{\vec{K}+\vec{k}}, b^\dagger_{-\vec{K}+\vec{k}})$ for small $\vec{k}$. Working to linear order in the lattice distortion and to linear order in $\vec{k}$, we find that the magnon Hamiltonian can be written as [19]

$$\mathcal{H}_{\mathrm{SW}} = 3JS\int d^2r \Psi^\dagger \begin{pmatrix} 1+a & -\frac{a_0}{2}(\Pi_x - i\Pi_y) \\ -\frac{a_0}{2}(\Pi_x + i\Pi_y) & 1+a \end{pmatrix}\Psi \quad (6)$$

where $\vec{\Pi} = \vec{p} + \vec{A}$ and $p_x = -i\partial_x$, $p_y = -i\partial_y$. Here, $a = -\beta(u_{xx} + u_{yy})/2$ encodes the strain-induced change of the magnon bandwidth, and the strain-induced gauge field $\vec{A}$ has the form

$$\vec{A} = \frac{\beta}{2a_0}\begin{pmatrix} u_{xx} - u_{yy} \\ -2u_{xy} \end{pmatrix} + \vec{A}_K. \quad (7)$$

This consists of a β-dependent part responsible for Landau-level physics [2,5] and a β-independent lattice correction $\vec{A}_K$ [23,24] which will be neglected in the following, for

details see Ref. [19]. In the unstrained case, $\vec{A}=0$ and $a=0$, and the spectrum of the Hamiltonian (6) can be obtained by Fourier and Bogoliubov transformations as $\omega_k = 3JS(1-k^2a_0^2/8)$, consistent with Eq. (3) for $\vec{q}=\vec{K}+\vec{k}$ and small $\vec{k}$.

The Hamiltonian (6) differs in three crucial points from other realizations of strain-induced gauge fields: (i) It describes bosonic quasiparticles, not fermionic electrons. (ii) Particle number is not conserved. As a result, a bosonic Bogoliubov transformation is required to diagonalize (6), technically different from the diagonalization of a Hermitian matrix. (iii) The diagonal elements in (6) are nonzero, as a result of magnon on-site energies.

We now solve the problem explicitly for triaxial strain (4) where $a=0$ by symmetry, and the β-dependent part of the vector potential reads $\vec{A}=2\beta\bar{C}(y/a_0,-x/a_0)^T$ corresponding to symmetric gauge.

We introduce two types of bosonic ladder operators

$$\alpha=\left[p_x+y\frac{2C}{a_0^2}+i\left(p_y-x\frac{2C}{a_0^2}\right)\right]\frac{a_0}{\sqrt{8C}}, \tag{8}$$

$$\gamma=\left[p_x-y\frac{2C}{a_0^2}-i\left(p_y+x\frac{2C}{a_0^2}\right)\right]\frac{a_0}{\sqrt{8C}}, \tag{9}$$

which obey $[\alpha,\alpha^\dagger]_-=[\gamma,\gamma^\dagger]_-=1$ and $[\alpha^{(\dagger)},\gamma^{(\dagger)}]_-=0$, and we have assumed $C>0$. The Hamiltonian now reads

$$\mathcal{H}_{\mathrm{SW}}=3JS\int d^2r\Psi^\dagger(\vec{r})\begin{pmatrix}1 & -\sqrt{2C}\alpha^\dagger\\ -\sqrt{2C}\alpha & 1\end{pmatrix}\Psi(\vec{r}). \tag{10}$$

As usual for Landau levels in symmetric gauge, the spectrum is determined by the α boson operators, whereas the γ boson operators commute with the α and the Hamiltonian, such that all single-particle levels display an extensive degeneracy corresponding to $m=\gamma^\dagger\gamma$.

The single-particle (magnon) eigenstates can be obtained from (10) by a bosonic Bogoliubov transformation [25]. The solutions of the corresponding differential equations can be written in real space as [19]

$$\Phi^{\pm}_{n,m}=\begin{pmatrix}c_n^{\pm}\phi_{n,m}\\ \phi_{n-1,m}\end{pmatrix},\qquad \Phi^{+}_{0,m}=\begin{pmatrix}\phi_{0,m}\\ 0\end{pmatrix}, \tag{11}$$

with integer quantum numbers $n\geq 1$ and $m\geq 0$. The wave functions $\phi_{n,m}$ are harmonic-oscillator eigenstates with $\phi_{n,m}=(n!m!)^{-1/2}(\alpha^\dagger)^n(\gamma^\dagger)^m\phi_0$ with $\alpha\phi_0=\gamma\phi_0=0$, in real space $\phi_0(r)\propto\exp[-Cr^*r/(4a_0^2)]$ where $r=x+iy$, and the coefficients are $c_n^+=\sqrt{2/(Cn)}$ and $c_n^-=\sqrt{Cn/2}$. Hence, we have a single set of $n=0$ solutions and paired sets of solutions with $n=1,2,3,\ldots$. The Hamiltonian (10) is diagonalized by magnon operators $A^{\pm}_{n,m}=\int d^2r\Psi^T(r)\Phi^{\pm}_{n,m}(r)$ and takes the Landau-level form

$$\mathcal{H}_{\mathrm{SW}}=\sum_m\left(E_0(A^+_{0,m})^\dagger A^+_{0,m}+\sum_{n=1,\pm}^{\infty}E_n(A^{\pm}_{n,m})^\dagger A^{\pm}_{n,m}\right) \tag{12}$$

up to a global constant. The magnon energies are

$$E_n=3JS\sqrt{1-2Cn}\approx 3JS(1-Cn),\quad n=0,1,2,\ldots \tag{13}$$

valid near the upper end of the spectrum, i.e., $Cn\ll 1$.

Equation (13) is our key result: The E_n represent the energies of highly degenerate magnon pseudo-Landau levels. In contrast to strained graphene, the Landau-level energy decreases with increasing Landau-level index n and the levels are equally spaced—the latter is related to the unstrained spectrum being quadratic (as opposed to linear) in momentum.

Emergent supersymmetry.—Given that the solutions for $n=1,2,\ldots$ occur in pairs, the degeneracy of the $n>0$ magnon Landau levels is twice as large as that of the $n=0$ level. This implies an emergent supersymmetry; i.e., the single-particle states can be mapped to that of a supersymmetric harmonic oscillator.

We can make this apparent by noting that the single-particle states (11), with energies (13), are the eigenstates of the following Hamiltonian:

$$h=3JS[1-C(F^\dagger F+B^\dagger B)], \tag{14}$$

where we have introduced the operators

$$F=\sum_m\sum_{n=0}^{\infty}|\Phi^+_{n,m}\rangle\langle\Phi^-_{n+1,m}|, \tag{15}$$

$$B=\sum_m\left(\sum_{n=0}^{\infty}\sqrt{n}|\Phi^+_{n,m}\rangle\langle\Phi^+_{n+1,m}|+\sum_{n=1}^{\infty}\sqrt{n}|\Phi^-_{n,m}\rangle\langle\Phi^-_{n+1,m}|\right), \tag{16}$$

which act in the single-particle Hilbert space; see Fig. S1 [19]. The $|\Phi^+_{0,m}\rangle$ and $|\Phi^{\pm}_{n,m}\rangle$ are (normalized) states corresponding to the real-space representation (11), with their scalar product defined via a Σ norm [19]. These states form a complete single-particle basis, and the operators F and B obey the canonical commutation relations for fermions and bosons, respectively, $[F,F^\dagger]_+=1$ and $[B,B^\dagger]_-=1$ [19].

Since both the boson (B) and the fermion (F) have the same excitation energy, Eq. (14) resembles an inverted supersymmetric harmonic oscillator. We emphasize that the supersymmetry arises from the two-sublattice structure combined with the nonconservation of the bosonic particle number: While the fermionic two-sublattice case yields a

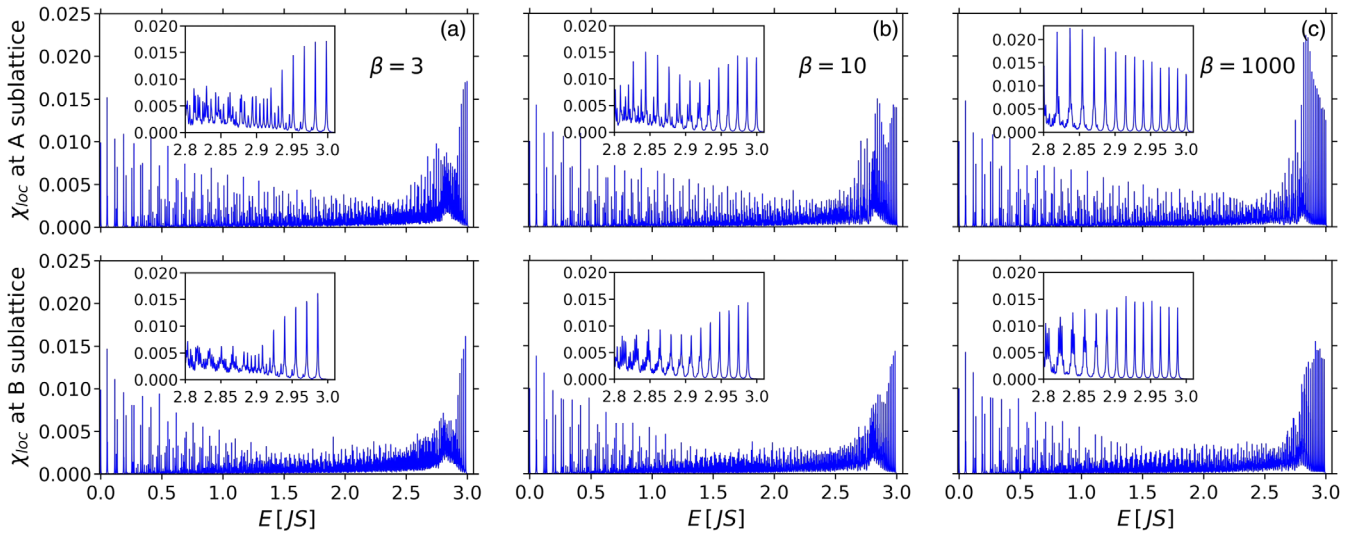

FIG. 2. Simulation results. Local susceptibility near the sample center on the A (top) and B (bottom) sublattices, obtained for $N = 100$, $C/C_{\max} = 0.4$ and different values of β. A Lorentzian broadening of $\eta = 10^{-4}JS$ has been applied. The insets show the upper end of the spectrum, with clearly visible pseudo-Landau levels.

spectrum which is particle-hole symmetric, the bosonic case requires non-negative excitation energies, then implying pairs of degenerate solutions for $n > 0$.

Numerical results.—To verify our field-theoretic calculation, we now turn to a numerical analysis of the magnon Hamiltonian on finite strained systems. In principle, arbitrarily shaped systems with open boundary conditions can be considered; guided by the insights of Ref. [14], we choose triangular-shaped systems with linear size N and N^2 sites, as shown in Fig. 1(a). We employ exchange couplings according to Eqs. (4) and (5), yielding a spin-wave Hamiltonian as in Eq. (2). We solve the bosonic Bogoliubov problem, amounting to the diagonalization of a non-Hermitian matrix of size $N^2 \times N^2$, using the algorithm outlined in the Appendix of Ref. [25].

For given system size N, the strain $C = \bar{C}\beta a_0$ has a maximum value $C_{\max}$ beyond which some of the exchange couplings become negative due to the linearization in (5). Hence, we parametrize the strain by its strength $C/C_{\max}$ and consider different values of the magnetoelastic coupling β. In general, the pseudomagnetic field will be spatially inhomogeneous, with variations near the edges, and clear Landau-level signatures are expected in the bulk of the sample [18].

Results for the local magnetic susceptibility, equivalent to the local magnon density of states (DOS), measured near the center of the sample, are shown in Fig. 2. Equally spaced Landau levels are clearly visible at the upper end of the spectrum in perfect agreement with Eq. (13), with the $n = 0$ level being present only on the A sublattice [19]. The Landau-level spacing scales linearly with applied strain [19] as anticipated. Note that the states at the lower spectrum end display small degeneracies only, see also Fig. 3 below, and do not correspond to Landau levels [19], except for the special case in Fig. 3(c).

As observed in Ref. [26] and discussed in detail in Ref. [14], the combined limit of large β and small $\bar{C}$ reduces nonlinearities in the pattern of bond strengths, such that pseudo-Landau levels can exist over a large range of energies. For this (artificial) $\beta \to \infty$ limit we show results

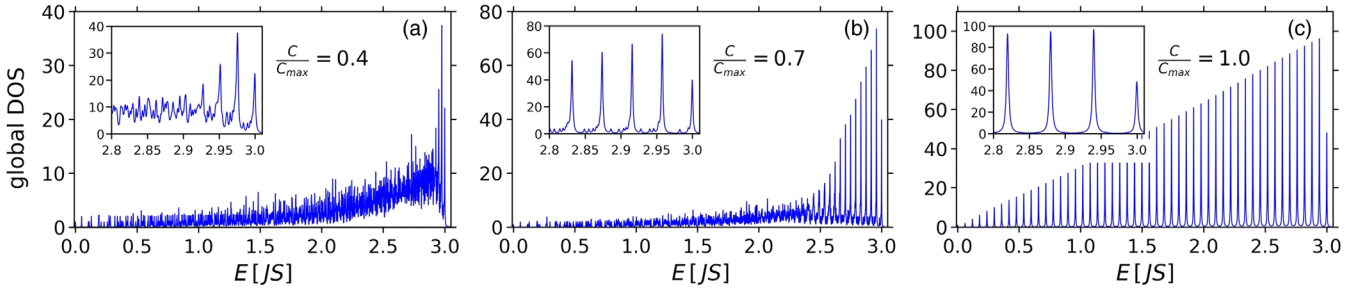

FIG. 3. Simulation results. Global magnon density of states, obtained for $N = 50$, $\beta = 1000$ and different values of $C/C_{\max}$. A Lorentzian broadening of $\eta = 10^{-3}JS$ has been applied [$\eta = 1.5 \times 10^{-3}JS$ in (c)]. The insets show the upper end of the spectrum, with the Landau-level spacing scaling linearly with $C/C_{\max}$.

for the global magnon DOS in Fig. 3. Most remarkable is the result for $C = C_{\max}$, Fig. 3(c), where we find perfectly degenerate and equally spaced magnon levels over the full bandwidth. For a system of linear size N there are $N+1$ magnon energies, $E_n = 3JS(1-n/N)$, with degeneracies $d_0 = N-1$, $d_N = 1$, and $d_n = 2(N-n)$ for $n = 1, \ldots, N-1$. For large N and small n, these degeneracies agree with the field-theoretic result derived above and reflect the supersymmetric nature of the spectrum. For $C < C_{\max}$, Figs. 3(a) and 3(b), the energy range of clearly visible magnon Landau levels decreases. Moreover additional peaks appear in between the Landau levels which correspond to magnon states localized near the sample edges, i.e., reflect finite-size effects [19].

Discussion.—Having established the existence of magnon Landau levels in strained honeycomb antiferromagnets, we turn to broader aspects. First, our calculation is controlled in the semiclassical limit of large spin S. Quantum (i.e., $1/S$) corrections lead to higher-order magnon terms in the Hamiltonian. In the present case with collinear order, cubic vertices are forbidden. Self-energy effects from quartic magnon interactions will shift all excitation modes at the upper end of the spectrum in a similar fashion, such that the Landau-level structure remains intact. Broadening effects arising from quartic vertices are typically small. While a full calculation is beyond the scope of this paper, we expect our results to be robust down to $S = 1/2$. Second, the Landau quantization implies that the semiclassical trajectory of a magnon wave packet centered at $\vec{K}$ or $\vec{K}'$ is a circle [27].

The experimental realization of Fig. 1(a) requires one to prepare a strained quasi-2D antiferromagnet and to measure its dynamic spin susceptibility. Although challenging, we believe this can be achieved with present-day technology: van-der-Waals–bonded layered magnets such as α-$RuCl_3$, $CrCl_3$, or CrI_3 can be prepared as ultrathin (even monolayer) samples. Those can be placed on a curved substrate surface to realize suitable strain, akin to what has been done for graphene [3]. The excitation spectrum of such a sample may be probed using inelastic Raman scattering or electron-spin-resonance techniques. Realistic values of $\beta = 3, \ldots, 5$ and $\bar{C} \lesssim 0.2/(Na_0)$ imply a Landau-level spacing of $10^{-3}J$ for a system of 500^2 atoms. Alternatively, a strained antiferromagnet may be realized in a cold-atom quantum simulator. This requires one to generate a Hubbard model in the Mott regime [28] on a suitable inhomogeneous optical lattice. More generally, all quantum simulators for fermionic Hubbard models could in principle be used [29], in particular, when an arbitrary two-dimensional lattice can be simulated [30].

Summary.—We have demonstrated how to engineer a novel state of matter, where magnon excitations of a collinearly ordered antiferromagnet display highly degenerate Landau levels at the top of the spectrum. This realization of strain-induced Landau levels fundamentally differs from previous ones, as the starting spectrum displays a quadratic (instead of linear) dispersion. Consequently, the spectrum features equidistant Landau levels, and moreover realizes emergent supersymmetry. We have also discovered that the combined limit of strong magnetoelastic coupling and weak lattice deformations leads to perfectly quantized magnon Landau levels over the full range of magnon energies.

Generalizations to other lattice structures will be discussed elsewhere. We anticipate that adapting the scheme developed in Ref. [14] will enable us to engineer magnon Landau levels also in collinear diamond-lattice antiferromagnets. Strain engineering of noncollinear antiferromagnets [31] will not only modify the excitation spectrum but also lead to strain-dependent reference states, possibly generating entirely new types of order. This exciting phenomenology is left for future work.

We thank D. Arovas, J. Attig, L. Fritz, I. Goethel, A. Rosch, and S. Trebst for discussions as well as collaborations on related work. We acknowledge financial support from the DFG through SFB 1143 (Project No. 247310070) and the Würzburg-Dresden Cluster of Excellence on Complexity and Topology in Quantum Matter—*ct.qmat* (EXC 2147, Project No. 39085490) as well as by the IMPRS on Chemistry and Physics of Quantum Materials. S. R. acknowledges the support of an ARC Future Fellowship (FT180100211).

[1] H. Suzuura and T. Ando, Phys. Rev. B **65**, 235412 (2002).
[2] F. Guinea, M. I. Katsnelson, and A. K. Geim, Nat. Phys. **6**, 30 (2010).
[3] N. Levy, S. A. Burke, K. L. Meaker, M. Panlasigui, A. Zettl, F. Guinea, A. H. Castro-Neto, and M. F. Crommie, Science **329**, 544 (2010).
[4] F. Guinea, A. K. Geim, M. I. Katsnelson, and K. S. Novoselov, Phys. Rev. B **81**, 035408 (2010).
[5] M. Vozmediano, M. Katsnelson, and F. Guinea, Phys. Rep. **496**, 109 (2010).
[6] J. Dalibard, F. Gerbier, G. Juzeliūnas, and P. Öhberg, Rev. Mod. Phys. **83**, 1523 (2011).
[7] M. Aidelsburger, S. Nascimbene, and N. Goldman, C.R. Phys. **19**, 394 (2018).
[8] G. Massarelli, G. Wachtel, J. Y. T. Wei, and A. Paramekanti, Phys. Rev. B **96**, 224516 (2017).
[9] E. M. Nica and M. Franz, Phys. Rev. B **97**, 024520 (2018).
[10] S. Rachel, L. Fritz, and M. Vojta, Phys. Rev. Lett. **116**, 167201 (2016).
[11] P. Kulish and E. Sklyanin, Zap. Nauchn. Semin. LOMI **95**, 129 (1980); J. Sov. Math. **19**, 1596 (1982).
[12] T. Grover, D. N. Sheng, and A. Vishwanath, Science **344**, 280 (2014).
[13] S.-K. Jian, C.-H. Lin, J. Maciejko, and H. Yao, Phys. Rev. Lett. **118**, 166802 (2017).
[14] S. Rachel, I. Göthel, D. P. Arovas, and M. Vojta, Phys. Rev. Lett. **117**, 266801 (2016).

[15] K. Nakata, S. K. Kim, J. Klinovaja, and D. Loss, Phys. Rev. B **96**, 224414 (2017).
[16] Y. Ferreiros and M. A. H. Vozmediano, Phys. Rev. B **97**, 054404 (2018).
[17] In the semiclassical limit, $S \to \infty$, the Hamiltonian (1) on the honeycomb lattice has a Néel ground state for any choice of $J_{ij} > 0$ which follows from energy minimization.
[18] M. Neek-Amal, L. Covaci, K. Shakouri, and F. M. Peeters, Phys. Rev. B **88**, 115428 (2013).
[19] See Supplemental Material at http://link.aps.org/supplemental/10.1103/PhysRevLett.123.207204, which includes Refs. [20–22], for a derivation of the continuum field theory, an illustration of the supersymmetric nature of the spectrum, a discussion of the effect of strain on the Goldstone modes, and for additional numerical results.
[20] A. H. Castro Neto, F. Guinea, N. M. R. Peres, K. S. Novoselov, and A. K. Geim, Rev. Mod. Phys. **81**, 109 (2009).
[21] V. M. Pereira and A. H. Castro Neto, Phys. Rev. Lett. **103**, 046801 (2009).
[22] M. M. Fogler, F. Guinea, and M. I. Katsnelson, Phys. Rev. Lett. **101**, 226804 (2008).
[23] A. L. Kitt, V. M. Pereira, A. K. Swan, and B. B. Goldberg, Phys. Rev. B **85**, 115432 (2012).
[24] M. R. Masir, D. Moldovan, and F. M. Peeters, Solid State Commun. **175–176**, 76 (2013).
[25] S. Wessel and I. Milat, Phys. Rev. B **71**, 104427 (2005).
[26] C. Poli, J. Arkinstall, and H. Schomerus, Phys. Rev. B **90**, 155418 (2014).
[27] M. M. Nayga *et al.* (to be published).
[28] D. Greif, M. F. Parsons, A. Mazurenko, C. S. Chiu, S. Blatt, F. Huber, G. Ji, and M. Greiner, Science **351**, 953 (2016).
[29] T. Hensgens, T. Fujita, L. Janssen, X. Li, C. J. Van Diepen, C. Reichl, W. Wegscheider, S. Das Sarma, and L. M. K. Vandersypen, Nature (London) **548**, 70 (2017).
[30] J. Salfi, J. A. Mol, R. Rahman, G. Klimeck, M. Y. Simmons, L. C. L. Hollenberg, and S. Rogge, Nat. Commun. **7**, 11342 (2016).
[31] J. Attig and S. Trebst, Phys. Rev. B **96**, 085145 (2017).